JACS
JOURNAL OF THE AMERICAN CHEMICAL SOCIETY
Communication
pubs.acs.org/JACS

Light Emission as a Probe of Energy Losses in Molecular Junctions

Oleksii Ivashenko,[†] Adam Johan Bergren,[*,‡] and Richard L. McCreery[*,†,‡]

[†]Department of Chemistry, University of Alberta, 11421 Saskatchewan Dr., Edmonton, Alberta T6G 2M9, Canada
[‡]National Institute for Nanotechnology, 11421 Saskatchewan Dr., Edmonton, Alberta T6G 2M9, Canada

Supporting Information

ABSTRACT: Visible light emission was observed for molecular junctions containing 5−19 nm thick layers of aromatic molecules between carbon contacts and correlated with their current−voltage behaviors. Their emission was compared to that from Al/AlOx/Au tunnel junctions, which has been previously attributed to transport of carriers across the AlOx layer to yield "hot carriers" which emit light as they relax within the Au contact. The maximum emitted photon energy is equal to the applied bias for the case of coherent tunneling, and such behavior was observed for light emission from AlOx and thin (<5 nm) molecular junctions. For thicker films, the highest energy observed for emitted photons is less than eV_{app} and exhibits an energy loss that is strongly dependent on molecular layer structure and thickness. For the case of nitroazobenzene junctions, the energy loss is linear with the molecular layer thickness, with a slope of 0.31 eV/nm. Energy loss rules out coherent tunneling as a transport mechanism in the thicker films and provides a direct measure of the electron energy after it traverses the molecular layer. The transition from elastic transport in thin films to "lossy" transport in thick films confirms that electron hopping is involved in transport and may provide a means to distinguish between various hopping mechanisms, such as activated electron transport, variable range hopping, and Poole Frankel transport.

Charge transport in nanoscale molecular junctions and single molecules with transport distances in the range from <1 to 25 nm has been studied extensively and shown to differ significantly from that in thicker organic films used in organic electronics.[1−5] Quantum mechanical tunneling is often invoked to explain transport in single molecules and in organic films with thickness <5 nm.[6−10] A transition from tunneling to other transport mechanisms has been noted for thicker devices, and proposals for this "beyond tunneling" regime include activated hopping[6,11−15] and field ionization.[16−18] While hopping is often proposed to explain long-range transport in both molecular and organic electronics, there are several different hopping mechanisms, including redox exchange, variable range hopping, multistep tunneling, and others. These hopping mechanisms are generally distinguished by their dependence on thickness, temperature, and applied voltage.[12,16]

We have reported extensively on carbon-based molecular junctions ranging in thickness from 1 to 22 nm, consisting of aromatic molecules bonded to conducting carbon substrates with top contacts of Cu or carbon.[16,19−23] Transport in such junctions has the exponential thickness dependence and temperature independence consistent with tunneling provided the transport distance is <∼5 nm.[8,20,22,24] However, molecular junctions of bisthienylbenzene (BTB) with a thickness (d) range from 4 to 22 nm showed transport behavior distinct from tunneling, with two regimes having attenuation coefficients (β) of 3.0 ± 0.3 nm^{-1} for d = 4−8 nm and 1.0 ± 0.2 nm^{-1} for 8−22 nm, observed over a wide temperature range from <10 to 300 K.[16] High current densities (e.g., 4 A/cm^2 at 2 V) at temperatures below 10 K indicate transport is "activationless" with a low-temperature Arrhenius slope of <0.5 meV. This behavior is not consistent with any of the classical transport mechanisms and was attributed to field ionization of the BTB molecules to generate carriers.

Light emission from inorganic tunnel junctions[25−27] and in scanning tunneling microscopy[28−30] has been reported and attributed to "hot" electrons reaching a metal contact and then undergoing photoemission. This process differs fundamentally from that occurring in organic light emitting diodes (OLEDs), since hot electron emission is a distinct mechanism from the electron/hole recombination occurring in OLEDs. Light emission from hot electrons in molecular junctions has not been reported to our knowledge, and the few analogous examples from inorganic materials are dominated by Al/AlOx devices.[31−33] Here, we show that light emission not only occurs in carbon-based molecular junctions but also provides a direct measure of energy losses occurring during charge transport. We show how hot carrier-induced light emission can be used as a type of "energy loss spectroscopy," providing information about carrier energetics not available from the external circuit, and which should be valuable for deducing transport mechanism(s). Of particular interest are the transition from tunneling to hopping with increasing device thickness and the nature of the hopping operative for various molecular junction structures. As described below, the energy loss depends strongly on molecular structure and is an example of a "molecular signature" relating molecular structure to electronic behavior.

All-carbon molecular junctions were fabricated as described previously,[21] with one exception regarding the substrate. A patterned SiOx/Cr/Au substrate with 30 nm Au thickness was covered by a 10 nm thick layer of electron-beam deposited carbon (eC) in order to reduce ohmic potential losses in the pyrolyzed photoresist films used previously.[34,35] Molecular layers were deposited on the Au/eC substrate by electrochemical reduction of diazonium reagents, and the molecular layer thickness was determined with AFM "scratching" as described

Received: September 23, 2015
Published: January 8, 2016

DOI: 10.1021/jacs.5b10018
J. Am. Chem. Soc. 2016, 138, 722−725

previously.[36] The top contact was 3 nm of eC followed by 20−30 nm of Au, deposited sequentially without breaking vacuum. Al/AlOx/Au and Al/AlOx/eC/Au tunnel junctions were made by thermal oxidation of 40 nm thick Al films on SiOx followed by deposition of a top contact through a shadow mask. The AlOx thickness was ∼4 nm, and thicknesses of component layers are indicated by subscripts, e.g., $Al_{40}/AlOx_4/Au_{30}$. Light emission was observed with a 50× microscope objective (NA = 0.45) that was coupled to a CCD/spectrograph by a fiber optic cable. DC bias was applied to molecular junctions with a Keithley 2602A sourcemeter operating in 4-wire mode. Transmission by the optics and the response of the back-thinned CCD detector limited the usable spectral response to 350−900 nm. Additional experimental details are included in Supporting Information (SI).

Current density vs applied voltage (J−V) curves are shown in Figure 1 for the junctions studied, which included Al/AlOx/Au

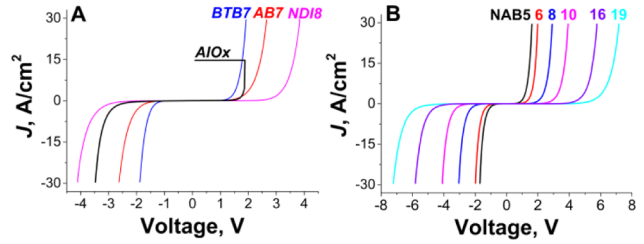

Figure 1. J−V curves for $Al/AlOx_4/Au_{30}$ and Au_{30}/eC_{10}/ molecule/ eC_3/Au_{30} junctions (thickness in nm indicated). (A) BTB_7, AB_7, and NDI_8, and AlOx. The AlOx device broke down at +1.6 V. (B) NAB from 5 to 19 nm.

and Au_{30}/eC_{10}/molecule/eC_3/Au_{20} junctions containing multilayers of bisthienylbenzene (7 nm, BTB_7), azobenzene (7 nm, AB_7), a naphthalene di-imide derivative[37] (8 nm, NDI_8), and nitroazobenzene (NAB) with thicknesses of 5, 6, 8, 10, 16, and 19 nm. In all cases, V_{app} is the bias at the substrate electrode relative to the top contact, with light emission observed through the top contact. When Al in Al/AlOx/Au is biased positive, breakdown occurs for V_{app} >∼1.6 V, presumably due to oxidation or electromigration of the Al contact. The J−V curves for molecular devices shown in Figure 1 are nearly symmetric with polarity and show a strong thickness dependence and nonlinear response described in previous reports on charge transport through molecular multilayers in the 2−22 nm thickness range.[8,16,19−21]

Light emission from Al/AlOx/Au tunnel junctions is well established and was used initially to develop the instrument and junction design. Figure 2A shows the emission spectra for V_{app} = −1.8 to −3.8 V (i.e., Al electrode negative), from the same junction that produced the Al/AlOx J−V curve in Figure 1. Note

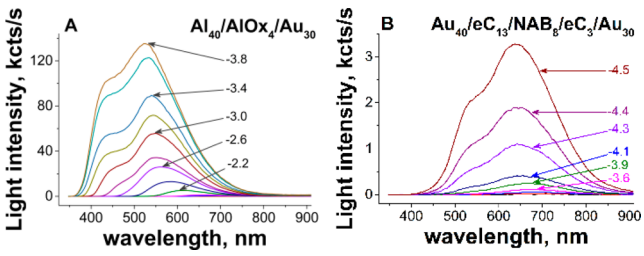

Figure 2. Emission spectra (uncorrected) for (A) $AlOx_4$ and (B) NAB_8 with $-V_{app}$ indicated (i.e., the substrate was negative in all cases). The intensity is given as the readout of a silicon CCD detector.

that the maximum photon energy increases with more negative V_{app} and that the emitted intensity increases with junction current. Past reports have associated photoemission from Al/AlOx/Au devices with "hot" electrons entering the top contact (Au) with excess energy relative to the contact Fermi level.[25−27] Coupling to plasmons in the Au then generates a photon as the electron loses energy in the Au contact.[32,33] The dip in emission at ∼450 nm has been attributed to interband transitions in Au.[38] The shape of the emission spectrum is a complex function of the plasmonic properties of the contact material, the dielectric properties of the layers, the viewing angle, etc., but emitted photon energy cannot exceed eV_{app}, the energy of the electron traversing the molecular layer. Note that the Au contact is capable of emitting photons over at least the range from 350 nm (3.5 eV) to 900 nm (1.4 eV), but that this range is "cut off" ($h\nu_{co}$) by the applied bias to a maximum energy of eV_{app}. For tunneling, transport is elastic, and electrons at the Al Fermi level arrive at the Au with excess energy relative to the Au Fermi level equal to eV_{app}. A plot of the cutoff energy, $h\nu_{co}$ vs eV_{app} should therefore be linear with a slope of 1.0 in the case of tunneling or other types of elastic transport. Figure 3A shows the experimental $h\nu_{co}$ vs eV_{app}

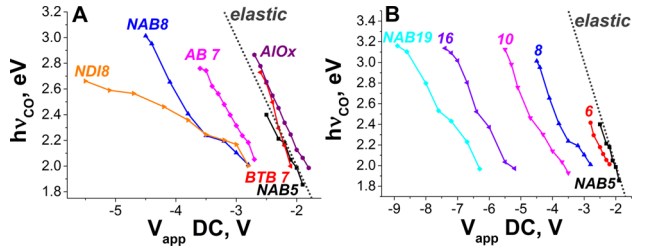

Figure 3. $h\nu_{co}$ as a function of V_{app} for (A) junctions with different molecular structures of similar thickness (the dashed line represents $h\nu_{co}$ = eV_{app}, and AlOx is shown for comparison) and (B) NAB junctions of varying thickness.

plot for AlOx, which has a slope of 1.00 ± 0.02. The offset to higher energy compared to the "elastic" line is physically unlikely and possibly due to the Fermi distribution of electrons in the Al or to experimental error in the determination of $h\nu_{co}$ (see SI).

Figure 2B shows emission spectra for the $Au_{30}/eC_{10}/NAB_8/eC_3/Au_{30}$ junction that exhibited the J−V curve shown in Figure 1B. All experimental parameters for voltage control and light detection were the same as those used for Al/AlOx/Au. Although it is possible to construct NAB junctions with Au top contacts and observe light emission (see SI, Figure 8), the yield and lifetime are low, presumably due to Au penetration into the NAB film as well as Au electromigration. Note also that emission from the NAB molecular junctions is significantly weaker than that from Al/AlOx, which may be partially due to eCarbon damping of the surface plasmons that mediate light emission. Given the negative substrate bias, light emission could result from electron transport from the substrate through the molecular layer to the top contact followed by light emission within the contact. Since the photoemission spectrum arises from plasmonic light generation in a metallic contact, its shape is not expected to vary greatly with molecular structure. However, the onset voltage and currents of photoemission depend strongly on molecular structure and thickness, as described next.

Spectra similar to those shown in Figure 2 were obtained for molecular junctions with the same Au_{30}/eC_{10}/ molecule/eC_3/Au_{20} composition but different molecular layer structures and thicknesses. The emission curves were obtained from the same

DOI: 10.1021/jacs.5b10018
J. Am. Chem. Soc. 2016, 138, 722−725

devices that produced the $J-V$ curves shown in Figure 1 in all cases. The structures, spectra, and thickness determination for these cases are provided in SI, and the electronic behaviors of junctions with thicknesses <5 nm have been described previously.[8,19,20] Figure 3A shows plots of $h\nu_{co}$ vs V_{app} for several examples, including molecular junctions from AB, NDI, and BTB with thicknesses of 7−8 nm. The "elastic" line represents the case where $h\nu_{co} = eV_{app}$ and indicates the maximum photon energy corresponding to elastic or tunneling transport. Note that emission from $AlOx_4$, BTB_7, and NAB_5 devices is close to the elastic limit, implying that at least some of the electrons crossing the junction do so without energy loss. In contrast, NAB_8, AB_7, and NDI_8 devices show a significant offset from the elastic line, indicating that carriers have lost energy during transport across the junction or alternatively that hot carriers with less than eV_{app} of energy are generated by field ionization within the organic layer. Stated differently, the average electron energy that can be generated in the device is eV_{app}, with a range of ±25 meV due to the Fermi distribution. Since the thicker junctions emit photons with significantly less energy than eV_{app}, the difference between eV_{app} and $h\nu_{co}$ represents the total loss of energy that occurs preceding observable photoemission. Note that the magnitude and slope of the plots in Figure 3A differ significantly for four junctions with nearly the same molecular layer thickness (NAB_8, BTB_7, AB_7, NDI_8). As shown in Figure 3B, the offset increases with increasing layer thickness for NAB films from 5 to 19 nm. Photoemission by molecular junctions represents a type of "energy loss spectroscopy", with some important consequences for deducing electron-transport mechanisms, as described below. Since $h\nu_{co}$ is the maximum energy of carriers reaching the top contact, the energy loss is readily determined as $eV_{app} - h\nu_{co}$. It should be kept in mind that this expression applies to the most energetic carriers reaching the top contact. The shape and magnitude of the emission spectra at energies below $h\nu_{co}$ are determined by many factors already noted, hence the transport analysis was based solely on $h\nu_{co}$ and eV_{app}.

Figure 4A is a plot of energy loss for selected junctions as a function of the applied bias. The thinnest devices (NAB_5, BTB_7, and AlOx) exhibit energy losses within ±0.2 eV of the elastic limit, and the energy loss is weakly dependent on bias. As noted above, the anomalous behavior of BTB_7 is currently unexplained, but the offsets from the elastic limit are much smaller than those for other molecules of similar thickness or for devices thicker than 7 nm. The remaining devices (NAB_6, AB_7, NAB_8, and NDI_8) all show larger losses than the "elastic" cases, and the loss increases with V_{app}. Figure 4A provides strong evidence that charge transport of carriers with energies sufficient to stimulate light emission is a function of molecular structure and that energy losses are a fundamental part of the transport mechanism for devices with layer thicknesses >∼5−7 nm (the specific range depends on molecular structure). Figure 4B shows the observed energy loss as a function of thickness of NAB and BTB junctions, with V_{app} selected as the onset voltage for light emission. The loss is linear with molecular layer thickness, with slopes of 0.31 and 0.15 eV/nm for NAB and BTB, respectively. The slopes of the plots therefore contain information about the facility with which each molecular structure can generate carriers that arrive at the top contact through whatever transport mechanism is responsible for transport. Inspection of Figure 4B also shows that the lines intersect near the elastic limit (i.e., zero on the ordinate) for a thickness of ∼5 nm, consistent with a change in mechanism from elastic to lossy transport at this distance. Thus, analysis of the characteristics of light emission from molecular junctions can provide information about both the nature of transport in molecular devices and the length at which transitions in transport mechanisms occur.

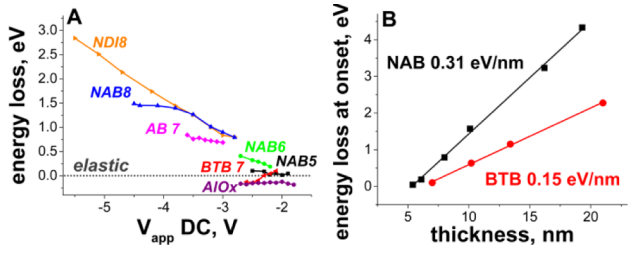

Figure 4. (A) Energy loss ($eV_{app} - h\nu_{co}$) as a function of V_{app} for the indicated junctions. (B) Energy loss at V_{app} corresponding to the onset of detectable light emission vs molecular layer thickness for BTB and NAB molecular junctions. Slope of each line is indicated.

Several observations about the light emission results are important to determining the charge-transport mechanism. First, light emission is a direct probe of the energy of electrons reaching the top contact, hence the term "energy loss spectroscopy." The shape of the emitted photon spectrum is more dependent on the contact material than the molecular layer structure, but nevertheless $h\nu_{co}$ indicates the maximum energy of carriers reaching the contact. Second, light emission for AlOx and thin molecular junctions (NAB_5 and BTB_7) exhibits minimal energy loss which depends weakly on bias, hence the transport is elastic. Many authors have discussed "coherent tunneling" and "incoherent" or "multistep" tunneling, depending on phase preservation during transport.[39−41] The elastic transport observed here could be either coherent or multistep, but at least it conserves the electron energy for molecular layers of ≤6 nm thickness. Previous reports on many molecular junctions with d = 2−5 nm showed that transport in thin junctions is weakly dependent on molecular structure, with similar attenuation coefficients of $\beta = 2.6 \pm 0.6$ nm for seven different aromatic molecules in this thickness range.[20] Third, the energy losses observed for thicker molecular junctions (Figures 3 and 4) clearly rule out coherent or "single step" tunneling as a transport mechanism. In any proposed "hopping" mechanism, there must be a means to account for the observed difference in energy between eV_{app} and $h\nu_{co}$. Fourth, the observed energy loss is strongly dependent on molecular structure for films thicker than 5−7 nm, and such devices also show much larger variation in $J-V$ behavior with structure than the 2−5 nm films reported previously[42] (Figure 1A). Whatever the charge-transport mechanism in the thicker films, these results imply that control of transport with structure is possible. Finally, the losses of 0.15−0.31 eV/nm observed for BTB and NAB are reasonable given the high electric fields of 2−5 MV/cm across the molecular layers and may support field ionization[16] or other transport modes not observed in organic electronics, where local electric fields are generally much lower.

Figure 5 shows an energy level diagram that summarizes the origin of light emission in carbon-based molecular junctions, based on the current results. Through further analysis involving characterization of light emission with systematic variation of bias voltage, thickness, molecular structure, and temperature, we anticipate additional conclusions about transport mechanisms and the nature of any hopping "sites".

DOI: 10.1021/jacs.5b10018
J. Am. Chem. Soc. 2016, 138, 722−725

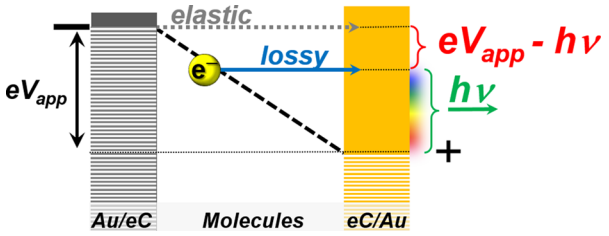

Figure 5. Electron transfer in molecular junctions can be elastic ("lossless") and inelastic ("lossy"). Relaxing to the Fermi level of the top contact results in light emission with energy ($h\nu$) that is directly related to the energy of carriers arriving at the contact.

■ ASSOCIATED CONTENT

Supporting Information

The Supporting Information is available free of charge on the ACS Publications website at DOI: 10.1021/jacs.5b10018.

Detailed experimental procedures, data, and figures (PDF)

■ AUTHOR INFORMATION

Corresponding Authors

*Adam.Bergren@nrc.ca

*Richard.McCreery@ualberta.ca

Notes

The authors declare the following competing financial interest(s): AJB and RLM have equity positions exceeding 5% in Nanolog Audio, Inc, which makes and sells molecular junctions for audio processing applications. The company's research and business are unrelated to the current manuscript, and Nanolog Audio did not provide financial support for the reported research.

■ ACKNOWLEDGMENTS

This work was supported by the University of Alberta, the National Research Council of Canada, the National Science and Engineering Research Council and Alberta Innovates Technology Futures. We thank Amin Morteza Najarian, Mykola Kondratenko, Akhtar Bayat, and Jerry Alfred Fereiro for the synthesis of diazonium salts used for fabrication of MJs and Nikola Pekas for valuable discussion. We thank Prof Jean-Christophe Lacroix for providing the BTB amine precursor used to prepare BTB molecular junctions.

■ REFERENCES

(1) Amdursky, N.; Marchak, D.; Sepunaru, L.; Pecht, I.; Sheves, M.; Cahen, D. *Adv. Mater.* **2014**, *26*, 7142.

(2) McCreery, R.; Yan, H.; Bergren, A. *Phys. Chem. Chem. Phys.* **2013**, *15*, 1065.

(3) Vilan, A.; Yaffe, O.; Biller, A.; Salomon, A.; Kahn, A.; Cahen, D. *Adv. Mater.* **2010**, *22*, 140.

(4) Salomon, A.; Cahen, D.; Lindsay, S.; Tomfohr, J.; Engelkes, V. B.; Frisbie, C. D. *Adv. Mater.* **2003**, *15*, 1881.

(5) Heath, J. R. *Annu. Rev. Mater. Res.* **2009**, *39*, 1.

(6) Choi, S. H.; Kim, B.; Frisbie, C. D. *Science* **2008**, *320*, 1482.

(7) Akkerman, H. B.; Naber, R. C. G.; Jongbloed, B.; van Hal, P. A.; Blom, P. W. M.; de Leeuw, D. M.; de Boer, B. *Proc. Natl. Acad. Sci. U. S. A.* **2007**, *104*, 11161.

(8) Bergren, A. J.; McCreery, R. L.; Stoyanov, S. R.; Gusarov, S.; Kovalenko, A. *J. Phys. Chem. C* **2010**, *114*, 15806.

(9) Engelkes, V. B.; Beebe, J. M.; Frisbie, C. D. *J. Am. Chem. Soc.* **2004**, *126*, 14287.

(10) Har-Lavan, R.; Yaffe, O.; Joshi, P.; Kazaz, R.; Cohen, H.; Cahen, D. *AIP Adv.* **2012**, *2*, 012164.

(11) Selzer, Y.; Cabassi, M. A.; Mayer, T. S.; Allara, D. L. *J. Am. Chem. Soc.* **2004**, *126*, 4052.

(12) Luo, L.; Choi, S. H.; Frisbie, C. D. *Chem. Mater.* **2011**, *23*, 631.

(13) Choi, S. H.; Risko, C.; Delgado, M. C. R.; Kim, B.; Bredas, J.-L.; Frisbie, C. D. *J. Am. Chem. Soc.* **2010**, *132*, 4358.

(14) Hines, T.; Diez-Perez, I.; Hihath, J.; Liu, H.; Wang, Z.-S.; Zhao, J.; Zhou, G.; Müllen, K.; Tao, N. *J. Am. Chem. Soc.* **2010**, *132*, 11658.

(15) Fan, F.-R. F.; Yao, Y.; Cai, L.; Cheng, L.; Tour, J. M.; Bard, A. J. *J. Am. Chem. Soc.* **2004**, *126*, 4035.

(16) Yan, H.; Bergren, A.; McCreery, R.; Della Rocca, M.; Martin, P.; Lafarge, P.; Lacroix, J. *Proc. Natl. Acad. Sci. U. S. A.* **2013**, *110*, 5326.

(17) Bof Bufon, C. C.; Vervacke, C.; Thurmer, D. J.; Fronk, M.; Salvan, G.; Lindner, S.; Knupfer, M.; Zahn, D. R. T.; Schmidt, O. G. *J. Phys. Chem. C* **2014**, *118*, 7272.

(18) DiBenedetto, S. A.; Facchetti, A.; Ratner, M. A.; Marks, T. J. *J. Am. Chem. Soc.* **2009**, *131*, 7158.

(19) Fereiro, J.; Kondratenko, M.; Bergren, A. J.; McCreery, R. L. *J. Am. Chem. Soc.* **2015**, *137*, 1296.

(20) Kane, E. O. *Phys. Rev.* **1962**, *127*, 131.

(21) Yan, H.; Bergren, A. J.; McCreery, R. L. *J. Am. Chem. Soc.* **2011**, *133*, 19168.

(22) McCreery, R. L.; Bergren, A. J. *Adv. Mater.* **2009**, *21*, 4303.

(23) McCreery, R. L.; Wu, J.; Kalakodimi, R. P. *Phys. Chem. Chem. Phys.* **2006**, *8*, 2572.

(24) Anariba, F.; Steach, J.; McCreery, R. *J. Phys. Chem. B* **2005**, *109*, 11163.

(25) Lambe, J.; Mccarthy, S. L. *Phys. Rev. Lett.* **1976**, *37*, 923.

(26) Kirtley, J.; Theis, T. N.; Tsang, J. C. *Phys. Rev. B: Condens. Matter Mater. Phys.* **1981**, *24*, 5650.

(27) Kirtley, J. R.; Theis, T. N.; Tsang, J. C.; DiMaria, D. J. *Phys. Rev. B: Condens. Matter Mater. Phys.* **1983**, *27*, 4601.

(28) Berndt, R.; Gaisch, R.; Gimzewski, J. K.; Reihl, B.; Schlittler, R. R.; Schneider, W. D.; Tschudy, M. *Science* **1993**, *262*, 1425.

(29) Berndt, R.; Gaisch, R.; Schneider, W. D.; Gimzewski, J. K.; Reihl, B.; Schlittler, R. R.; Tschudy, M. *Appl. Phys. A: Solids Surf.* **1993**, *57*, 513.

(30) Gimzewski, J. K.; Sass, J. K.; Schlitter, R. R.; Schott, J. *Europhys. Lett.* **1989**, *8*, 435.

(31) Sparks, P. D.; Rutledge, J. E. *Phys. Rev. B: Condens. Matter Mater. Phys.* **1989**, *40*, 7574.

(32) Watanabe, J.; Uehara, Y.; Ushioda, S. *Phys. Rev. B: Condens. Matter Mater. Phys.* **1995**, *52*, 2860.

(33) Sparks, P. D.; Sjodin, T.; Reed, B. W.; Stege, J. *Phys. Rev. Lett.* **1992**, *68*, 2668.

(34) Bonifas, A. P.; McCreery, R. L. *Anal. Chem.* **2012**, *84*, 2459.

(35) Bonifas, A. P.; McCreery, R. L. *Chem. Mater.* **2008**, *20*, 3849.

(36) Anariba, F.; DuVall, S. H.; McCreery, R. L. *Anal. Chem.* **2003**, *75*, 3837.

(37) Fereiro, J.; McCreery, R. L.; Bergren, A. J. *J. Am. Chem. Soc.* **2013**, *135*, 9584.

(38) Dawson, P.; Walmsley, D. G.; Quinn, H. A.; Ferguson, A. J. L. *Phys. Rev. B: Condens. Matter Mater. Phys.* **1984**, *30*, 3164.

(39) Danilov, A.; Kubatkin, S.; Kafanov, S.; Hedegard, P.; Stuhr-Hansen, N.; Moth-Poulsen, K.; Bjornholm, T. *Nano Lett.* **2008**, *8*, 1.

(40) Aleshkin, V. Y.; Reggiani, L.; Rosini, M. *Phys. Rev. B: Condens. Matter Mater. Phys.* **2006**, *73*, 165320.

(41) Berlin, Y. A.; Grozema, F. C.; Siebbeles, L. D. A.; Ratner, M. A. *J. Phys. Chem. C* **2008**, *112*, 10988.

(42) Sayed, S. Y.; Fereiro, J. A.; Yan, H.; McCreery, R. L.; Bergren, A. J. *Proc. Natl. Acad. Sci. U. S. A.* **2012**, *109*, 11498.